Shedding a light on the physical stability of suspensions micronised with intensified vibratory milling; A trend observed with decreasing particle size as a function of time

De Cleyn, Elene; Holm, René; Van den Mooter, Guy

Published in:
International Journal of Pharmaceutics

DOI:
10.1016/j.ijpharm.2021.120687

Publication date:
2021

Document Version
Early version, also known as pre-print

Citation for published version (APA):
De Cleyn, E., Holm, R., & Van den Mooter, G. (2021). Shedding a light on the physical stability of suspensions micronised with intensified vibratory milling; A trend observed with decreasing particle size as a function of time. *International Journal of Pharmaceutics*, *603*, [120687]. https://doi.org/10.1016/j.ijpharm.2021.120687

Shedding a light on the physical stability of suspensions micronised with intensified vibratory milling; A trend observed with decreasing particle size as a function of time.

De, Cleyn E; Holm, R; Van, den Mooter G

Published in:
International Journal of Pharmaceutics

DOI:
10.1016/j.ijpharm.2021.120687

Publication date:
2021

Document version:
Submitted manuscript

Shedding a light on the physical stability of suspensions micronised with intensified vibratory milling;

***A trend observed with decreasing particle size as a function of time*.**

Contact:

Elene De Cleyn[1], René Holm[2, 3, 4], Guy Van den Mooter[1*]

[1] Drug Delivery and Disposition, Department of Pharmaceutical and Pharmacological Sciences, University of Leuven (KU Leuven), O&N II Herestraat 49 - box 921, 3000 Leuven, Belgium

[2] Drug Product Development, Janssen Research and Development, Johnson and Johnson, Turnhoutseweg 30, 2340 Beerse, Belgium

[3] Department of Science and Environment, Roskilde University, 4000 Roskilde, Denmark

[4] Department of physics, chemistry and pharmacy, University of Southern Denmark, Campusvej 55, 5230 Odense, Denmark

*Correspondence;

Guy Van den Mooter

O&N II Herestraat 49 -box 921, 3000 Leuven, Belgium

guy.vandenmooter@kuleuven.be,

tel.+32 16 33 03 04

tel. +32 473 356 132

LIST OF ABBREVIATIONS*

GRAPHICAL ABSTRACT

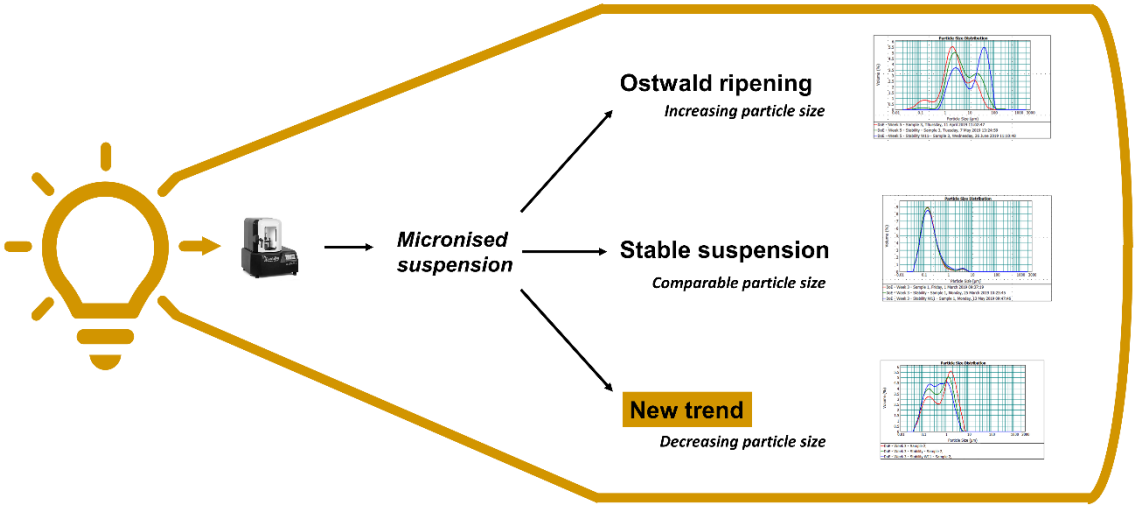

*API: Active pharmaceutical ingredient, DoE: Design of experiments, LD: Laser diffraction, Obsc.: Red light obscuration, Obsc. blue.: Blue light obscuration, PSD: Particle size distribution, iRI: imaginary part of the complex refractive index, rRI: Real part of the complex refractive index, Res.: Residuals, Res. Weight.: Residuals weighted, SEM: Scanning electron microscopy

1. ABSTRACT

Intensified vibratory milling is a nanonisation and micronisation technology which can be used to enable the oral bioavailability of poorly soluble compounds. The generated nano- and microsuspensions entail a large surface area which enhances the compounds dissolution rate, yet the suspensions have unfavourable effects and hence spontaneous destabilisation may occur, i.e. physical instability. Stability studies on suspensions manufactured via intensified vibratory milling have, to the best of our knowledge, not before been reported in the literature. An extended stability study was, therefore, executed with 30 bedaquiline suspensions milled with the intensified vibratory mill under various process settings. The particle size distribution was measured after production, four weeks of storage at 5°C and eleven weeks of storage at 5°C with laser diffraction and scanning electron microscopy. In addition, a caking test was applied to scrutinise the redispersibility of the prevailing sediments. One sample whose sediment proved to be redisperible, demonstrated a peculiar trend during storage where a narrowing of the particle size distribution and a general particle size reduction was detected which opposed the conventional stability tendencies, i.e. Ostwald ripening. This enigmatic trend was further explored via a repetitive analysis with laser diffraction and in a further phase, with an orthogonal particle sizing technique. Still, no matter the frequency nor technique, a narrowing particle size distribution was observed. To the best of our knowledge, this article, for the first time in the pharmaceutical literature, reports a narrowing particle size distribution of a micronised suspension containing an organic compound. Inevitably, this trend might shed a fundamental new light on the stability trends, exposed by suspensions post-micronisation by high energy milling.

2. INTRODUCTION

During the technological and scientific advances of the 1980s, two discovery platforms, were generated which led to a wide range of potential drug leads: combinatorial chemistry and high-throughput screening. Despite their high potential, most of these compounds exhibited a poor aqueous solubility and as a consequence, a poor and variable oral bioavailability.(Van Hijfte et al., 1999) Micro- and nanosuspensions have presented a strong marketable value in the formulation of these poorly soluble compounds, as their entailed large surface area enhances the compounds dissolution rate. Nevertheless, these suspensions are, *de facto,* thermodynamically unfavourable.(Fontana et al., 2018) (Wu et al., 2011) The stability of micro- and nanosuspensions is therefore continuously challenged by a multitude of destabilising phenomena, comprising sedimentation, Ostwald ripening, secondary nucleation and aggregation.(Wu et al., 2011) Sedimentation is the most abundant among particles larger than 5 µm. Provided that the sediment can be homogeneously redispersed, the settling process is not necessarily detrimental for the suspension's storage life. In this light, suspensions are often categorised in flocculated and deflocculated systems, where flocculated systems contain loose aggregates.(Kipp, 2004) Their sediment is easy to redisperse, but settles fast which restrains the time-window for accurate sampling or accurate patient dosing. Deflocculated systems gradually settle but their particles create a sturdy, non-dispersible, solid cake. Formulation scientists consequently aim for the midpoint of these two extremes, the partial or controlled flocculation, where the loose aggregates are still resuspendable and settle at an acceptable rate.(Joshi et al., 2002)

By virtue of Brownian motion, particles smaller than 5 µm may evade the sedimentation process but are, especially in the case of polydisperse systems, more prone to undergo Ostwald ripening; a process wherein large particles grow at the expense of smaller particles. A large body of literature suggests that an excess of stabiliser might promote Ostwald ripening, however, a more recent study of Verma and co-workers identified Ostwald ripening as a multi-step process whose rate controlling step will determine the optimal stabiliser concentration.(Ariyaprakai and Dungan, 2009) (Verma et al., 2011) Other nanoparticle growth pathways such as digestive ripening and intraparticle ripening may occasionally occur in inorganic materials but are only scarcely discussed

in pharmaceutical literature.(Thanh et al., 2014) There are, to the best of our knowledge, only two publications in the pharmaceutical literature reporting a particle size reduction of an active pharmaceutical ingredient (API) during storage. However, the API was in both occasions in the dry state.(Nyqvist and Wadsten, 1985) (Joshi et al., 2002)

It has been hypothesised that the manufacturing technology can impact the stability of the manufactured suspension (Wang et al., 2013), nonetheless, in-depth research on the topic is lacking. Hence, the purpose of the present study is to investigate the relationship between manufacturing on IVM and the stability of the produced suspensions.

3. MATERIALS AND METHODS

3.1. Materials

Bedaquiline was provided by Janssen Pharmaceutica (Beerse, Belgium). Polysorbate 20 was obtained from Croda (Trappes, France). Poloxamer 338 was obtained from BASF (Kolliphor® P338, BASF, USA). Deionised water (R≥18.2 MΩ, Mili-Q® Advantage A10, Merck, Darmstadt, Germany) was used for all the experiments.

3.2. Methods

3.2.1. Preparation of suspensions

Glass vials were filled with bedaquiline (5% w/v), zirconia beads (Nikkato Corporation, Sakai, Osaka, Japan) and polysorbate 20 solution (1.85 %w/v). The vials were thoroughly shaken on an in-house manufactured platform within the LabRAM II (Resodyn™ Acoustic Mixers, Butte, USA). The process parameters - the acceleration, the bead size, the bead-suspension ratio, the milling time and the breaks during milling - were varied as shown in Table 1.

Table 1. Overview of the process parameters applied during the production of the 30 samples of the first stability study.

Sample	Process Parameters				
Block 1	**Bead size (µm)**	**Bead-suspension ratio (mL/mL)**	**Acceleration (g)**	**Milling time (min)**	**Breaks during milling (min)**
Sample 1	200	0.375	50	10	2.5
Sample 2	200	1.200	50	10	0
Sample 3	1000	0.375	65	20	5
Sample 4	200	0.375	80	30	5
Sample 5	1000	0.774	80	30	2.5
Sample 6	1750	0.375	80	20	0
Block 2					
Sample 1	1000	1.200	50	20	2.5
Sample 2	1750	0.774	65	10	2.5
Sample 3	1750	1.200	80	10	5
Sample 4	1750	1.200	80	10	5
Sample 5	1750	0.774	65	10	2.5
Sample 6	1000	1.200	50	20	2.5
Block 3					

Sample 1	200	1.200	80	30	2.5
Sample 2	1000	1.200	80	10	0
Sample 3	1750	0.774	50	10	5
Sample 4	1750	0.375	50	30	2.5
Sample 5	1000	0.774	65	20	2.5
Sample 6	1750	0.375	50	10	0
Block 4					
Sample 1	1750	1.200	80	30	0
Sample 2	1000	0.774	65	20	2.5
Sample 3	1750	1.200	50	30	0
Sample 4	1750	0.375	80	10	5
Sample 5	200	1.200	65	20	0
Sample 6	1000	0.375	65	30	0
Block 5					
Sample 1	200	0.774	50	30	0
Sample 2	1750	0.774	65	30	5
Sample 3	200	0.774	50	30	0
Sample 4	200	0.774	80	10	5
Sample 5	200	1.200	50	30	5
Sample 6	200	0.375	80	10	0

3.2.2. Laser diffractometry

Mastersizer 2000™

In the Mastersizer 2000™ (Malvern Instruments, Worcestershire, UK) with hydro-unit, miliQ water was used as the dispersant. A stirring speed of 600 rpm was set, no sonication was applied, and the system was left to stabilise. The general-purpose model for irregularly shaped particles with normal calculation sensitivity was applied. The set optical parameters were a real part of the complex refractive index (rRI) of 1.595 for the sample, an imaginary part of the complex refractive index (iRI) of 0.001 for the sample and a dispersant rRI of 1.333. A limited obscuration titration was performed for each sample to elucidate the optimal set of red light (obsc.) and blue light obscuration (obsc. blue). Quality of data was given in terms of residuals (res.) and residuals weighted (res weight.), as described in prior work.(De Cleyn et al., 2019) The final particle size distribution (PSD) was described by the dv10-value, dv50-value and the dv90-value.

Mastersizer 3000™

In the Mastersizer 3000™ (Malvern Instruments, Worcestershire, UK) with hydro-unit, a 1% dilution of poloxamer 338 in miliQ water was used as the dispersant. A stirring speed of 2000 rpm was set, and no sonication was applied. The general-purpose model for irregularly shaped particles with normal calculation sensitivity was applied. The set optical parameters were rRI of 1.61, a sample iRI of 0.01 and a dispersant rRI of 1.333. As sample preparation, 0.1 mL of the suspension was diluted in 10 mL of miliQ water. The final PSD was described by the dv10-value, the dv50-value and the dv90-value.

3.2.3. Differential centrifugal sedimentation

The differential centrifugal sedimentation was performed on a CPS Instruments Disk Centrifuge (CPS Instruments, Inc. Prairieville, LA, USA), model DC24000 equipped with a normal density disc and detector at the wavelength of 405 nm, to obtain a weight-average PSD, described by the dw10-value, the dw50-value and the dw90-value. The disk centrifuge was operated at 20 000 rpm, and the spin fluid contained a sucrose density gradient (4% to 12%) which was refreshed every four hours. A calibration and a system suitability test with polyvinylchloride standards were executed prior to sample analysis. For the sample analysis, the particle density was set at 1.31 g/mL and the particle refractive index and particle absorption were set at 1.61 and 0.01, respectively. The sample was diluted prior to analysis, by the dispersion of 70 drops of the suspension, generated with a 23G needle, in 50 mL of miliQ water.

3.2.4. Scanning electron microscopy

Suspensions were diluted with miliQ water and consecutively dried on an Isopore filter (ø 0.100 µm). The filters were adhered to the scanning electron microscopy (SEM) stubs using double-sided carbon tape. All samples were gold coated with a Quorum Q150 R S gold sputter (Quorum Technologies Ltd, Laughton, East Sussex, England)

and placed within the Phenom Pro-X (ThermoFisher Scientific, MA, USA) to acquire the SEM images.

3.2.5. Caking test

For the caking test, the vials containing the samples were vigorously shaken to homogeneously disperse the suspension and to redisperse possible sediment. If a headspace was present, the vial was held upside down to control if a solid cake was even after agitation or still attached at the bottom of the vial. If this control was not attainable, the suspension was poured out to enable further investigation of the solid cake.

3.2.6. Stability study

Post-milling stability trends

The samples of the DoE (Table 1) were produced per block and stored after production at 5°C. To investigate their particle size and morphology, SEM pictures were taken just after production and after four weeks of storage. Further, a Mastersizer 2000™ particle size measurement was performed after production, after four and eleven weeks of storage at 5°C with exception of the samples of block 4 which were analysed after fifteen weeks instead of eleven weeks. The PSDs of each sample were superimposed within the Mastersizer 2000™ software to identify the stability trend of the sample, which subcategorised the samples in the following, four categories; i) the category ‘Stable’ referred to the stable suspensions whose PSDs minimally changed over time; ii) the category ‘Ostwald’ referred to the suspensions whose particle size clearly increased over time; iii) for the suspensions of the category ‘Unclear’, the variability of the laser diffraction (LD) data did not permit a clear identification of the stability trend and iv) the suspensions of the category ‘New trend’ demonstrated a peculiar particle size reduction during storage. The caking test was performed on all thirty samples at the end of the stability study, hence after the second stability measurement of the samples of block 5. At that point, samples were stored for 21 to 11 weeks, for block 1 to block 5, respectively.

Confirmation of the new trend

In a second study, the reproducibility of the previously mentioned ‘New trend’ was tested. The ‘New trend’ sample where no caking prevailed (Sample 2, Block 3, Table 3), was remanufactured in fourfold at two different time points, leading to two completely independent datasets. These sample sets were investigated with LD, SEM and the caking test on at least two different timepoints, as presented in Table 2.

Table 2. Overview of the timing and the analysis techniques applied to confirm the reproducibility of the new trend observed in sample 2 of block 3 of table 2.

	Sample set 1	**Sample set 2**
After production	Caking, SEM	LD, SEM
Timepoint 1	*4 weeks*: LD, Caking, SEM	*3 weeks:* LD, caking, SEM
Timepoint 2:	*7 weeks*: LD, Caking, SEM	/

In order to verify this new trend, the ‘New trend’ sample (Sample 2, Block 3, Table 3) was remanufactured in sixfold and divided in sets of three where one set was studied with the Mastersizer 2000™ and the other set was investigated with the Mastersizer 3000™ and differential centrifugal sedimentation after production, after four and ten weeks of storage at 5°C.

4. RESULTS AND DISCUSSION

4.1. Post-milling stability trends

Table 3. Overview of the stability trends of the 30 samples of the first stability study.

Sample	After production			After 4 weeks			After 11 weeks			Stability trend	Caking test
Block 1	**dv10 (µm)**	**dv50 (µm)**	**dv90 (µm)**	**dv10 (µm)**	**dv50 (µm)**	**dv90 (µm)**	**dv10 (µm)**	**dv50 (µm)**	**dv90 (µm)**		
Sample 1	3.469	21.125	64.279	3.553	21.194	55.701	4.147	26.549	75.073	Stable	No caking
Sample 2	0.335	3.97	40.469	0.849	3.699	37.467	1.137	4.332	43.17	Ostwald	No caking
Sample 3	0.154	1.657	4.27	0.165	1.346	3.306	0.195	1.43	3.426	Stable	No caking
Sample 4	0.118	0.637	22.695	0.128	0.808	8.733	0.148	1.05	24.646	Stable	No caking
Sample 5	0.096	0.376	1.746	0.101	0.316	0.932	0.096	0.333	1.512	Stable	No caking
Sample 6	0.148	1.918	4.924	0.105	0.374	1.288	***0.117***	***0.388***	***1.17***	New trend	***Caking***
Block 2	**dv10 (µm)**	**dv50 (µm)**	**dv90 (µm)**	**dv10 (µm)**	**dv50 (µm)**	**dv90 (µm)**	**dv10 (µm)**	**dv50 (µm)**	**dv90 (µm)**		
Sample 1	0.103	0.658	2.65	0.109	0.562	2.234	0.134	0.944	2.89	Ostwald	No caking
Sample 2	0.161	2.046	4.929	0.106	0.828	2.528	***0.191***	***1.445***	***3.86***	Unclear	***Caking***
Sample 3	0.126	1.34	4.025	0.102	0.515	2.341	***0.143***	***1.198***	***3.736***	Unclear	***Caking***
Sample 4	0.13	1.283	3.807	0.102	0.513	2.344	0.108	0.504	2.056	Unclear	No caking
Sample 5	0.153	1.768	4.152	0.11	0.798	2.529	***0.134***	***1.146***	***2.999***	Unclear	***Caking***
Sample 6	0.115	0.855	2.885	0.105	0.531	2.239	0.143	1.044	3.138	Unclear	No caking
Block 3	**dv10 (µm)**	**dv50 (µm)**	**dv90 (µm)**	**dv10 (µm)**	**dv50 (µm)**	**dv90 (µm)**	**dv10 (µm)**	**dv50 (µm)**	**dv90 (µm)**		
Sample 1	0.071	0.158	0.433	0.071	0.158	0.47	0.073	0.167	0.552	Stable	No caking
Sample 2	0.114	0.897	3.088	0.103	0.552	2.187	0.105	0.457	1.882	New trend!	No caking
Sample 3	0.167	1.946	4.509	0.273	1.62	3.494	***0.357***	***2.048***	***4.916***	Stable	***Caking***
Sample 4	0.137	1.736	4.13	0.124	0.935	2.56	***0.187***	***1.483***	***3.531***	Unclear	***Caking***
Sample 5	0.108	0.682	2.585	0.141	0.539	1.598	***0.115***	***0.792***	***2.672***	Stable	***Caking***

Sample 6	0.85	2.077	4.378	0.769	1.852	4.629	***1.322***	***3.349***	***9.369***	Ostwald	***Caking***
							Stability 15 weeks			**AFTER W 15 INSTEAD OF W11**	
Block 4	**dv10 (µm)**	**dv50 (µm)**	**dv90 (µm)**	**dv10 (µm)**	**dv50 (µm)**	**dv90 (µm)**	**dv10 (µm)**	**dv50 (µm)**	**dv90 (µm)**		
Sample 1	0.117	1.241	2.881	0.136	0.631	2.106	1.126	2.135	4.086	Ostwald	No caking
Sample 2	0.102	0.568	2.271	0.11	0.615	2.291	0.112	0.899	3.191	Unclear	No caking
Sample 3	0.105	0.516	2.287	0.108	0.434	1.95	0.115	0.817	3.146	Ostwald	No caking
Sample 4	0.154	1.958	4.437	0.226	1.669	6.157	***Caking***	***-***	***-***	Ostwald	***Caking***
Sample 5	0.081	0.213	0.898	0.085	0.239	2.642	0.091	0.299	30.997	Ostwald	No caking
Sample 6	0.134	1.184	3.286	0.113	0.486	1.724	***Caking***	***-***	***-***	Unclear	***Caking***
Block 5	**dv10 (µm)**	**dv50 (µm)**	**dv90 (µm)**	**dv10 (µm)**	**dv50 (µm)**	**dv90 (µm)**	**dv10 (µm)**	**dv50 (µm)**	**dv90 (µm)**		
Sample 1	0.669	4.855	48.012	1.368	5.684	44.419	1.724	18.109	63.181	Ostwald	No caking
Sample 2	0.114	0.908	3.225	0.108	0.418	1.61	0.146	0.813	2.506	Stable	No caking
Sample 3	0.467	2.651	18.444	1.252	4.848	34.698	1.698	14.891	61.028	Ostwald	No caking
Sample 4	0.101	0.414	4.081	0.111	0.611	5.338	0.12	0.724	4.589	Unclear	No caking
Sample 5	0.169	1.777	18.073	0.492	2.778	34.873	0.95	5.312	54.557	Ostwald	No caking
Sample 6	0.981	3.099	25.094	1.364	3.89	27.877	1.428	4.291	26.345	Stable	No caking

If caking was observed in a sample of block 1 to 3, inadequate sampling during particle size measurements might have occurred which would have resulted in invalid data. Thus, the results of the particle size measurement of the second stability point might be invalid and were therefore highlighted in bold, red and italic. If a solid cake was detected in a sample of block 4 or block 5, the second stability measurement was not performed.

The 30 samples did not only present different PSDs after production but demonstrated different stability trends (Figure S-1, Figure S-2, Figure S-3, Figure S-4, Figure S-5) as well, leading to their categorisation in four stability trends (Table 3). Even though PSDs and thus stability trends were confirmed by SEM, they were merely defined by LD data and their accuracy was therefore challenged by a caking test. The large volume of data extracted from this stability study (Table 3) impeded a broad, yet accurate discussion of each sample. Nonetheless, some peculiar trends were noted which will be detailed below.

Despite their identical formulation, suspensions with comparable PSDs after production could still demonstrate different stability trends, as displayed in sample 3 and sample 6 of block 1 in Table 3. They presented similar PSDs after production with a dv10-, dv50- and dv90-value of 0.154 µm, 1.657 µm, 4.27 µm, and, 0.148 µm, 1.918 µm, 4.29 µm, respectively. Nonetheless, the PSDs evolved differently during storage where sample 3 remained stable throughout the whole study whereas an indispersible cake materialised in sample 6. The temperature after production, retrieved as explained in prior work (De Cleyn et al., 2020) was distinct with a value of 40.1°C and 66.2°C for sample 3 and 6, respectively. As an increased temperature might lead to the (partial) desolvation of the hydrophilic part of the applied surfactant, it might have rendered its stabilisation efficacy. As a result, the attraction energy between two particles will prevail, and the particles will tend to aggregate. The higher temperature that sample 6 faced could therefore explain the poor stability outcome as compared to sample 3. From a stability point of view, these data suggested a preferred use of a moderate acceleration, a smaller and thus, in this case, more performant bead size and even intermittent pausing, as occurred during the production of sample 3. Milling at a higher acceleration without intermittent pausing as occurred during the manufacturing of sample 6, seemed less favourable. As proposed by Wang and co-workers(Wang et al., 2013), these findings suggest that the applied particle size reduction technology and even more, the applied process parameters, might impact the stability of the manufactured suspension. Furthermore, as formulation screenings are merely executed with fixed process settings, these findings highlight how formulation scientists should take the production technology and parameters in consideration when examining the results of such formulation screenings.

The most striking result from this dataset was the anomalous trend of a particle size reduction during storage, observed in a few samples of the stability study (‘New trend’, Table 3). This new trend was, as a first investigation, challenged via a caking test. As described by Stokes’ law, larger particles of a multidisperse system will settle faster than their smaller counterparts.(Wu et al., 2011) To render an indispersible cake where smaller particles need to settle in-between these sedimented larger particles, however, the smallest particles (mostly nanometer-range) will, by virtue of the Brownian motion, hardly settle, if at all. The undispersible sediment will therefore merely comprise of the larger particles of a multidisperse system. As these larger particles settle, the supernatans will increasingly contain smaller particles. Sampling often occurs in the supernatans, hence the measured PSD will become less and less representative for suspensions with aggregation behaviour and will thereby provide a false readout, i.e. a particle size reduction. Via the caking test, samples containing a solid, indispersible sediment were traced (Table 3) to ensure that the provided data was not affected by the phenomenon discussed above. The last stability data of the samples of block 1 to 3, were, as caking occurred, highlighted in bold, italic and red to indicate their possible inaccuracy. In the case of the samples of block 4 and 5, the particle size measurement was not executed if caking occured (Sample 4 and sample 6, Block 4, Table 3).

Suprisingly, sample 2 of block 3 did not demonstrate an indispersible sediment, however, it did present the new trend during storage (Figure 1). The change in the particle size distribution was confirmed via SEM, where the size distribution of the rather multidisperse particulate system seemed to narrow down as a function of time (Figure 2). The operating parameters to manufacture this suspension were an acceleration of 80 g, a milling time of 10 min, a bead-suspension ratio of 1.2 and a bead size of 1000 µm. The installed bead-suspension ratio and acceleration were rather harsh, though the milling time was limited to 10 minutes. With a final suspension temperature of 85 °C, heat was importantly generated. The final temperature was thus close to, yet did not surpass the cloud point of the stabiliser polysorbate 20 (ca. 97 °C) (Na et al., 1999). Partial dehydration could occur but aggregation was not observed in the SEM images. As this unexpected behaviour would shed a new light on the behaviour of suspensions after micronisation, an investigation of this particular trend was pursued.

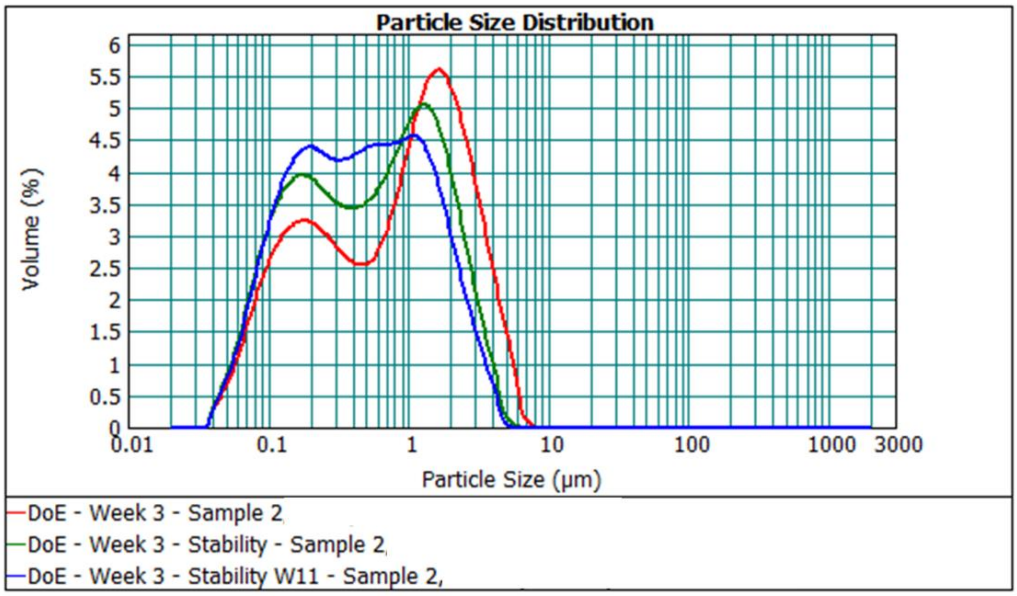

Figure 1. Particle size distributions of sample 2 of block 3 of table 2, after production (red curve), after four weeks of storage at 5 °C (green curve) and after eleven weeks of storage at 5°C (blue curve). A peculiar trend was observed where the portion of nanoparticles, as compared to the microparticles, seemed to increase over time.

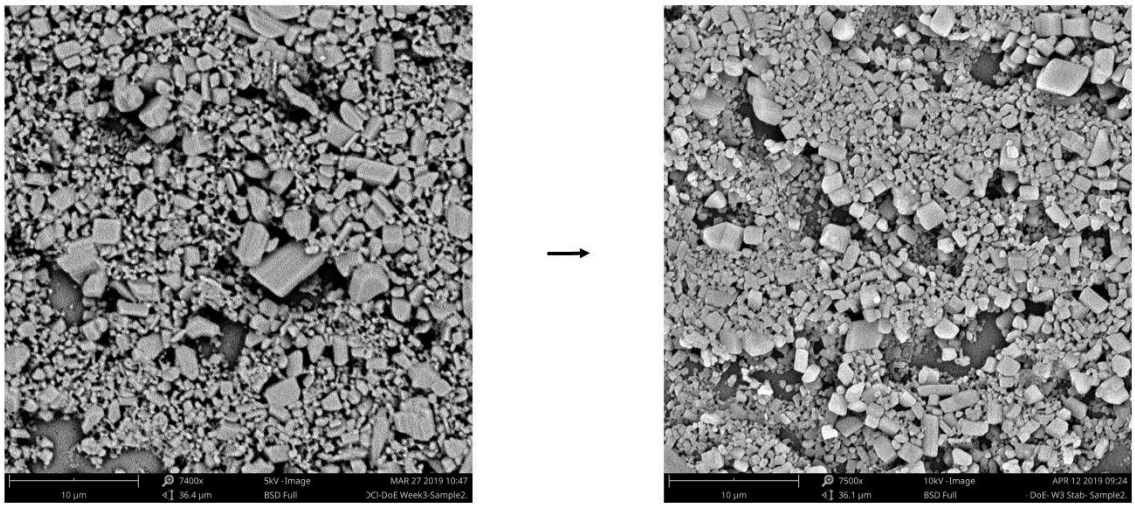

Figure 2. Change in particle size and morphology as observed in SEM for the sample 2 of block 3. The particle size distribution after production (left) seemed to be wider and seemed to contain a larger portion of bigger particles than the particle size distribution after four weeks of storage at 5 °C (right). In both cases, a polyhedral morphology was detected.

4.2. Confirmation of the new trend

Table 4. Investigation of the reproducibility of the particle size reduction during storage observed in sample 2 of block 3 of table 2.

Sample set	Stability point	dv10 (µm)	dv50 (µm)	dv90 (µm)
2	**After production**	0.109	0.939	3.568
2	**After three weeks**	0.122	0.541	1.99
1	**After four weeks**	0.13	0.573	2.175
1	**After seven weeks**	0.118	0.796	3.095

The particle sizes presented in this summarising table are the average values, measured with the Mastersizer 2000™. Sample set 2 was measured after production and after three weeks of storage at 5°C and sample set 1 was measured after four weeks and after seven weeks of storage at 5°C.

As a confirmation of the reproducibility of this stability trend, the investigated suspension (Sample 2, Block 3, Table 3) was remanufactured and followed over time. The caking test remained negative throughout the stability study, indicating that the suspension could be completely redispersed. The summarising results (Table 4) of the raw data (Table S-1, Table S-2, Table S-3, Table S-4), demonstrated the reproducibility of the observations. The dv50-value declined from a value of 0.939 µm to a value of 0.541 and 0.573 µm during the first three to four weeks of storage (Table 4). This particle size reduction was even more apparent in the dv90-value which sharply reduced to approximately half its original value. In the previous stability study the particle size continued to decrease over time, whereas the PSDs in this stability study presented a slight particle growth. Despite this difference in the second phase of the stability study, the net result remained the same. In both stability studies the PSDs at the end of the storage time were narrower and had a lower dv50-value than the PSDs just after production. In order to exclude that the trend was a reproducible flaw of the analysis technique, the Mastersizer 2000™, the trend was further studied using the Mastersizer 3000™ and an orthogonal particle size measurement technique namely differential centrifugal sedimentation.

Table 5. Summarising table presenting the average values and standard deviation of the particle size of three 'New trend' samples, measured with the Mastersizer 2000™, at three time points; after production, after four weeks of storage at 5°C and after ten weeks of storage at 5°C.

Storage		dv10 (µm)	dv50 (µm)	dv90 (µm)
0 weeks	**Average**	0.107	0.787	3.385
	Standard deviation	*0.007*	*0.113*	*0.103*
4 weeks	**Average**	0.148	0.626	2.194
	Standard deviation	*0.012*	*0.103*	*0.435*
10 weeks	**Average**	0.157	0.757	2.748
	Standard deviation	*0.024*	*0.128*	*0.227*

Table 6. Summarising table presenting the average values and standard deviation of the particle size of three 'New trend' samples, measured with the Mastersizer 3000™ at three time points; after production, after four weeks of storage at 5°C and after ten weeks of storage at 5°C.

Storage		dv10 (µm)	dv50 (µm)	dv90 (µm)
0 weeks	**Average**	0.353	1.170	3.223
	Standard deviation	*0.017*	*0.106*	*0.249*
4 weeks	**Average**	0.385	1.150	3.213
	Standard deviation	*0.019*	*0.050*	*0.167*
10 weeks	**Average**	0.279	0.866	2.920
	Standard deviation	*0.006*	*0.020*	*0.113*

Table 7. Summarising table presenting the average values and standard deviation of the particle size of three 'New trend' samples, measured with differential centrifugal sedimentation, at three time points; after production, after four weeks of storage at 5°C and after ten weeks of storage at 5°C.

Storage		dw10 (nm)	dw50 (nm)	dw90 (nm)
0 weeks	**Average**	208	592	1332
	Standard deviation	*11*	*17*	*110*
4 weeks	**Average**	196	509	1045
	Standard deviation	*7*	*36*	*161*
10 weeks	**Average**	196	506	1139
	Standard deviation	*6*	*35*	*62*

The PSDs observed with the Mastersizer 2000™ (Table 5, Table S-5) were comparable to the previously retrieved data. The Mastersizer 3000™ data (Figure 3, Table 6 and Table S-6) confirmed the particle size reduction from week zero to week four. However, in the second phase of the stability study a particle size decrease was detected by the Mastersizer 3000™ whereas a slight particle size increase was

detected by the Mastersizer 2000™. This difference may be attributed to the increased sensitivity of the Mastersizer 3000™ to nanoparticles, hence the Mastersizer 3000™ data were presumably more accurate. Still, the dv50-value in both the Mastersizer 2000™ and the Mastersizer 3000™ reduced during the entire stability study. This trend was further supported by the data acquired by differential centrifugal sedimentation (Figure 4, Table 7 and Table S-7). However, the particle sizes generated by differential centrifugal sedimentation were considerably smaller than the data obtained with LD. Yet, the dataset confirmed, the narrowing of the PSD over time. Moreover, similar stability trends were observed with other APIs as well (data non-disclosed). Even though this peculiar trend seemed very contraindicative towards the widely known and accepted stability trends for dispersed systems, it was repeatedly observed and confirmed by an orthogonal particle sizing technique in the present work. Based on physicochemical principles, a non-exhaustive list of plausible hypotheses is provided below, comprising digestive ripening or reversed Ostwald ripening, the crystallisation of the amorphous (regions on the) surface of the API particle, (surface) degradation and the Rehbinder effect. Discarded hypotheses included intraparticle ripening and a stabiliser enabled disaggregation, as will be explained below.

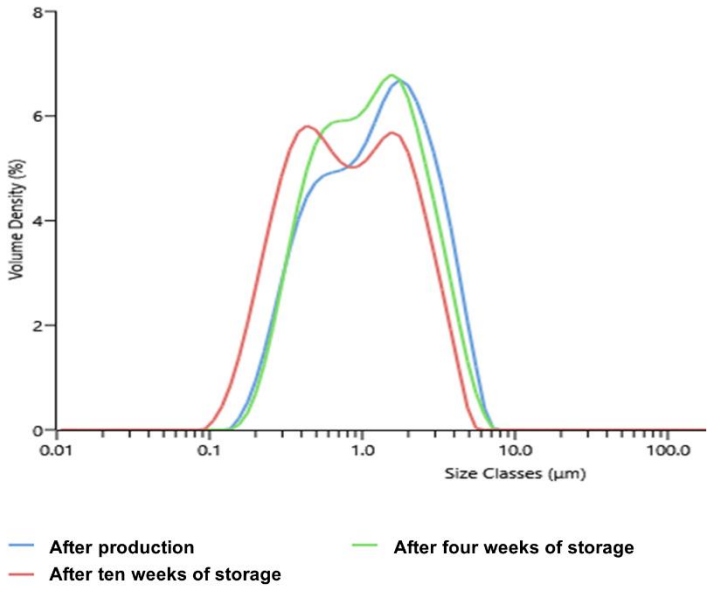

Figure 3. Particle size reduction of sample F, as observed in the Mastersizer 3000™, illustrated by the PSD after production (blue curve), after four weeks of storage (green curve) and after ten weeks of storage (red curve). The PSD after production contain larger particles which evolves to smaller sized PSD.

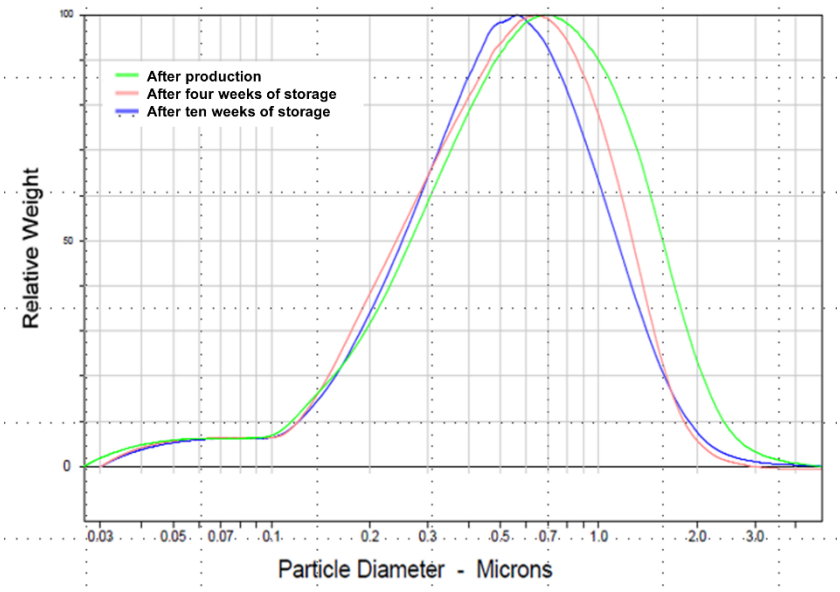

Figure 4. Particle size reduction of sample F, as observed with differential centrifugal sedimentation. Larger particles are present after production (green curve) which evolves to a smaller sized PSD after four weeks of storage at 5°C (red curve) and ten weeks of storage at 5°C (blue curve).

Within inorganic chemistry, the process in which smaller particles grow at the expense of larger particles is denoted as the process of digestive ripening or reversed-Ostwald ripening and has been the subject of extensive research.(Thanh et al., 2014) (Shimpi et al., 2017) How the size modification during reversed Ostwald ripening precisely occurs still remains to be elucidated and mainly descriptive insights are provided within inorganic chemistry.(Shimpi et al., 2017) A current working hypothesis is the existence of a region in the parameter space of component concentrations and interaction energies where smaller particles are more stable than their larger counterparts. By the addition of a surface energy lowering excipient, *e.g.* the wetting agent polysorbate 20, the effective surface energy of the small particles might become negative. Mass would transfer from the larger particles to these smaller particles and subsequently the PSD narrows to mono-sized particles.(Thanh et al., 2014) (Burlakov et al., 2014) (Burlakov and Goriely, 2020) Even though this theory appears particularly appealing to the investigated system consisting of an API and the stabiliser polysorbate 20, extreme caution must be paid in the direct translation of the given theorem. Contrary to the research carried out in the field, the rate of the phenomenon presented itself over weeks, whereas digestive ripening merely appears as a rapid process of maximum a few hours. Another disagreement is the particle size range in which the phenomenon

takes place. While in the field of inorganic chemistry digestive ripening applies to a few dozen of nanometres to quantum dots, the trend observed in our study was only present at the higher nano- and lower microscale.(Thanh et al., 2014) (Lee et al., 2007) Albeit, the most intriguing analogy of the surface energy lowering excipient, resuscitates digestive ripening as potential hypothesis.(Burlakov et al., 2014)

Other interpretations for this intriguing trend, are related to the surface of the API particle (Figure 5). As the IVM is a high intensity milling process, it might mechanically activate regions at the surface of the API and consequently reduce the crystallinity of the milled compound.(Wang et al., 2013)

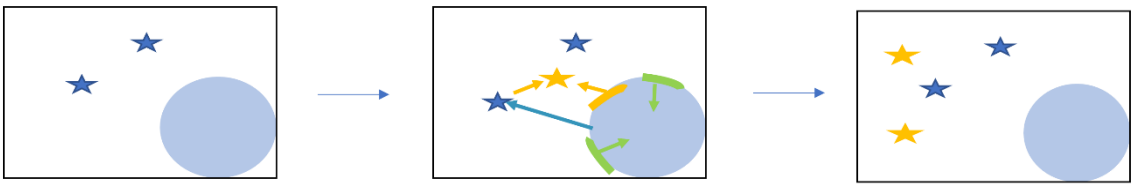

Figure 5. Surface phenomena that might occur during milling, illustrated by the circumstances before milling (left), immediately after milling (middle) and at a later time point after milling (right). Due to the high intensity milling, surface domains might amorphisize which might crystallise during storage causing a volume reduction (green arrows). Due to the high intensity milling, surface degradation may occur. The degradation product might have a higher solubility than its poorly soluble parent compound and might consequently dissolve in the suspension matrix (yellow arrows). Bedaquiline submicron suspensions are more prone to degradation than their macro-counterparts. As a result, degradation in the suspension matrix might shift equilibria to an extent that particles start to dissolve over time (yellow and blue arrows)

As a result, the crystal surface becomes disordered, which results in a highly defective crystal phase that may spontaneously convert to localised amorphous regions.(Wang et al., 2013) (Shah et al., 2015) As the amorphous compound is characterised by an enhanced solubility and a higher free energy, reordering of these crystal defects and crystallisation of the amorphous regions might spontaneously occur during storage. The high water content of the suspension matrix will act as a plasticiser, which undoubtedly will trigger this crystallisation process.(Wang et al., 2013) (Shah et al., 2015) causing a reduction of the particle volume and hence, an overall size reduction (Figure 5).(Chu and Steeves, 2011) However, previous findings in our group suggested that in the case of naproxen and cinnarizine amorphisation due to media milling is highly unlikely in the suspended state and that the occasionally detected amorphous fraction presumably originates form the drying process, required for solid-state

analysis. These findings were more specifically prevalent for APIs that had an increased solubility in the stabiliser, which complies to the herein studied system of bedaquiline and polysorbate 20.(Kayaert and Van Den Mooter, 2012)

Further, these amorphous regions show a higher reactivity which in the presence of an aqueous medium, may lead to chemical degradation, as observed for naproxen by other authors.(Kumar and Burgess, 2014) Furthermore, research in our group distinguished how cryomilling might trigger polymer and subsequentially API degradation.(Pas et al., 2020) Considering mechanical activation might occur in the highly energetic IVM as well, surface API may degrade, generating degradation products that might be more soluble than their poorly soluble parent compound. In these circumstances, the degradation product might dissolve in the aqueous environment, which drives particle size reduction (Figure 5).

Despite the stability of bedaquiline in solid or in dispersed state, the submicron suspension demonstrated an increased photodegradation (data non-disclosed). Provided that the degradants are more soluble than to the parent compound bedaquiline, photodegradation might shift the mass equilibria and drive a particle size reduction (Figure 5).

Another hypothesis is the propagation of the Rehbinder effect post-micronisation. During nano- and micronisation, the stabiliser plays a major role in the mechanical breakdown of the API via three different phenomena comprising the wetting and stabilisation of the newly formed surfaces, its contribution to the microhydrodynamics of the mixing and milling regime, and in the particle strength as described by the Rehbinder effect.(Monteiro et al., 2013) This Rehbinder effect explains how the stabiliser reduces the compound hardness which eventually leads to crack propagation.(Monteiro et al., 2013) (Erik Kissa, 1999) (Bhakay et al., 2011) The addition of a stabiliser enhances the wet breakage rage via both the Rehbinder effect and the wetting and stabilisation mechanism. However, as they coincidently occur, there is no consensus on which mechanism is more dominant. Attempts of Biligili and co-workers to address the question, led to two publications with contradictory findings.(Monteiro et al., 2013) (Bhakay et al., 2011) The increasing surface area of dry budesonide post-micronisation, was nonetheless clarified by the theories of stress relief and crack propagation (Joshi et al., 2002) Taken together, there is still

considerable controversy on the applicability of the Rehbinder effect in pharmaceutical wet milling kinetics. Bearing in mind that the crack propagation would, within the presented study, occur during storage, the hypothesis seemed highly doubtful as compared to other well-reasoned hypotheses. Albeit, Monteiro and co-workers described how the stabiliser sodium lauryl sulphate enabled the penetration of the suspension medium into the aggregate pores. The aggregates consequently disaggregated resulting in an apparent particle size reduction.(Monteiro et al., 2013) This theory could be transposed to our investigated system, but was discarded as the acquired SEM images did not display any (dis)aggregation behaviour.

Another interesting hypothesis, which was eventually discarded by the SEM observations and the orthogonal particle sizing technique, included intraparticle ripening; a process where monomers diffuse along the surface of nanoparticles to modify the particles habitus with time (Figure 6). The working hypothesis of intraparticle ripening is, as in the case of digestive ripening, based on the different surface energies of the various facets of an API particle.(Thanh et al., 2014) Another reasoning may be found in the Ostwald-Freundlich equation which denotes that the saturation solubility of a particle is highly dependent on its curvature.(Sandri et al., 2018) Following LDs assumption of particle sphericity, a change in habitus would importantly inflict LDs accuracy and might be erroneously captured as a particle size reduction. Still, no change in morphology was apparent on the SEM images (Figure 2). Furthermore, the enigmatic trend was confirmed via an orthogonal particle sizing technique.

Figure 6. Theoretical example of intraparticle dissolution, where the edges of a needle shaped particle dissolve and recrystallise on other facets of the API particle, changing the particles morphology from needle shape to spherical shape. From an LD perspective, this habitus change would be interpreted as a particle size reduction.

Even though a clear hypothesis could, at this point, not be provided, the novelty of the perceived stability trend encouraged an early publication. The herein provided datasets

and list of explanatory hypotheses form, in this way, a stimulus for future investigation as they shed a new light on suspensions post-micronisation behaviour.

5. CONCLUSIONS

The herein provided stability study contributed to the observation that the selected production technology and process parameters considerably affect the stability of the produced suspensions. As a result, the applied process technology and process parameters should be taken into consideration during a formulation screening as it is conventionally executed with fixed process settings. Furthermore, one manufactured suspension presented an unconventional narrowing of its particle size distribution over time which to the best of our knowledge have not been reported in the pharmaceutical literature before. This peculiar trend was further explored via a caking test, via repetitive measurements with laser diffraction and via an orthogonal particle sizing technique which all confirmed this enigmatic trend. More confirmatory experiments are, however, required. Due to the novelty of the presented post-milling behaviour, early data were already provided. A non-exhaustive list of hypothesises based on physicochemical principles provide the needed framework for further exploration.

6. ACKNOWLEDGEMENTS

We gratefully acknowledge Divya Bahadur for retrieving the Mastersizer 3000 data™. The authors also thank Linda Lauwerysen as she performed the differential centrifugal sedimentation experiments.

7. REFERENCES

Ariyaprakai, S., Dungan, S.R., 2009. Influence of surfactant structure on the contribution of micelles to Ostwald ripening in oil-in-water emulsions. J. Colloid Interface Sci. 343, 102–108. https://doi.org/10.1016/j.jcis.2009.11.034

Bhakay, A., Merwade, M., Bilgili, E., Dave, R.N., 2011. Novel aspects of wet milling for the production of microsuspensions and nanosuspensions of poorly water-soluble drugs. Drug Dev. Ind. Pharm. 37, 963–976. https://doi.org/10.3109/03639045.2010.551775

Burlakov, V.M., Bootharaju, M.S., Besong, T.M.D., Bakr, O.M., Goriely, A., D Besong, T.M., Bakr, O.M., Goriely, A., 2014. Reversing Ostwald Ripening, arxiv.org.

Burlakov, V.M., Goriely, A., 2020. Reverse coarsening and the control of particle size distribution through surfactant. Appl. Sci. 10, 5359. https://doi.org/10.3390/APP10155359

Chu, J.J., Steeves, C.A., 2011. Thermal expansion and recrystallization of amorphous Al and Ti: A molecular dynamics study. J. Non. Cryst. Solids 357, 3765–3773. https://doi.org/10.1016/j.jnoncrysol.2011.07.019

De Cleyn, E., Holm, R., Khamiakova, T., Van den Mooter, G., 2021. Picking up good vibrations:Exploration of the intensified vibratory mill via a modern Design of Experiments. Int. J. Pharm. 120367. https://doi.org/10.1016/j.ijpharm.2021.120367

De Cleyn, E., Holm, R., Van den Mooter, G., 2020. Exploration of the heat generation within the intensified vibratory mill. Int. J. Pharm. 587, 119644. https://doi.org/10.1016/j.ijpharm.2020.119644

De Cleyn, E., Holm, R., Van den Mooter, G., 2019. Size Analysis of Small Particles in Wet Dispersions by Laser Diffractometry: A Guidance to Quality Data. J. Pharm. Sci. 108, 1905–1914. https://doi.org/10.1016/j.xphs.2018.12.010

Erik Kissa, 1999. 7.I.C. Effect of dispersant on communition, in: Kissa, E. (Ed.), Dispersions: Characterization, Testing, and Measurement -.

Fontana, F., Figueiredo, P., Zhang, P., Hirvonen, J.T., Liu, D., Santos, H.A., 2018.

Production of pure drug nanocrystals and nano co-crystals by confinement methods. Adv. Drug Deliv. Rev. 131, 3–21. https://doi.org/10.1016/J.ADDR.2018.05.002

Joshi, V., Dwivedi, S., Ward, G.H., 2002. Increase in the specific surface area of budesonide during storage postmicronization. Pharm. Res. 19, 7–12. https://doi.org/10.1023/A:1013690929173

Kayaert, P., Van Den Mooter, G., 2012. Is the amorphous fraction of a dried nanosuspension caused by milling or by drying? A case study with Naproxen and Cinnarizine. Eur. J. Pharm. Biopharm. 81, 650–656. https://doi.org/10.1016/j.ejpb.2012.04.020

Kipp, J.E.E., 2004. The role of solid nanoparticle technology in the parenteral delivery of poorly water-soluble drugs. Int. J. Pharm. 284, 109–122. https://doi.org/10.1016/j.ijpharm.2004.07.019

Kumar, S., Burgess, D.J., 2014. Wet milling induced physical and chemical instabilities of naproxen nano-crystalline suspensions. Int. J. Pharm. 466, 223–232. https://doi.org/10.1016/j.ijpharm.2014.03.021

Lee, D.K., Park, S. Il, Lee, J.K., Hwang, N.M., 2007. A theoretical model for digestive ripening. Acta Mater. 55, 5281–5288. https://doi.org/10.1016/j.actamat.2007.05.048

Monteiro, A., Afolabi, A., Bilgili, E., 2013. Continuous production of drug nanoparticle suspensions via wet stirred media milling: A fresh look at the Rehbinder effect. Drug Dev. Ind. Pharm. 39, 266–283. https://doi.org/10.3109/03639045.2012.676048

Na, G.C., Yuan, B.O., Stevens, Jr., H.J., Weekley, B.S., Rajagopalan, N., Stevens, H.J., Weekley, B.S., Rajagopalan, N., 1999. Cloud point of nonionic surfactants: modulation with pharmaceutical excipients. Pharm. Res. 16, 562–568. https://doi.org/10.1023/A:1018831415131

Nyqvist, H., Wadsten, T., 1985. Can ageing effects in drugs be measured and interpreted by ta-techniques? Thermochim. Acta 93, 125–127. https://doi.org/10.1016/0040-6031(85)85032-2

Pas, T., Smeets, B., Ramon, H., Van Schepdael, A., Mansour, M., Koekoekx, R., Clasen, C., Vergauwen, B., Van Den Mooter, G., 2020. Mechanodegradation of Polymers: A Limiting Factor of Mechanochemical Activation in the Production of Amorphous Solid Dispersions by Cryomilling. Mol. Pharm. 17, 2987–2999. https://doi.org/10.1021/acs.molpharmaceut.0c00376

Sandri, G., Bonferoni, M.C., Rossi, S., Caramella, C.M., Ferrari, F., 2018. Effects of particle size, surface nature and crystal type on dissolution rate, in: AAPS Advances in the Pharmaceutical Sciences Series. Springer Verlag, pp. 303–328. https://doi.org/10.1007/978-3-319-94174-5_8

Shah, U. V., Wang, Z., Olusanmi, D., Narang, A.S., Hussain, M.A., Tobyn, M.J., Heng, J.Y.Y., 2015. Effect of milling temperatures on surface area, surface energy and cohesion of pharmaceutical powders. Int. J. Pharm. 495, 234–240. https://doi.org/10.1016/j.ijpharm.2015.08.061

Shimpi, J.R., Sidhaye, D.S., Prasad, B.L. V., 2017. Digestive Ripening: A Fine Chemical Machining Process on the Nanoscale. Langmuir 33, 9491–9507. https://doi.org/10.1021/acs.langmuir.7b00193

Thanh, N.T.K., Maclean, N., Mahiddine, S., 2014. Mechanisms of Nucleation and Growth of Nanoparticles in Solution. Chem. Rev. 114, 7610–7630. https://doi.org/10.1021/cr400544s

Van Hijfte, L., Marciniak, G., Froloff, N., 1999. Combinatorial chemistry, automation and molecular diversity: New trends in the pharmaceutical industry. J. Chromatogr. B Biomed. Sci. Appl. https://doi.org/10.1016/S0378-4347(99)00007-9

Verma, S., Kumar, S., Gokhale, R., Burgess, D.J., 2011. Physical stability of nanosuspensions: Investigation of the role of stabilizers on Ostwald ripening. Int. J. Pharm. 406, 145–152. https://doi.org/10.1016/J.IJPHARM.2010.12.027

Wang, Y., Zheng, Y., Zhang, L., Wang, Q., Zhang, D., 2013. Stability of nanosuspensions in drug delivery. J. Control. Release 172, 1126–1141. https://doi.org/10.1016/j.jconrel.2013.08.006

Wu, L., Zhang, J., Watanabe, W., 2011. Physical and chemical stability of drug

nanoparticles. Adv. Drug Deliv. Rev. 63, 456–469.
https://doi.org/10.1016/j.addr.2011.02.001